Cumhuriyet Sci. J., 46(2) (2025) 310-318
DOI: https://doi.org/10.17776/csj.XXXXXXX

Cumhuriyet Science Journal

| csj.cumhuriyet.edu.tr | Founded: 2002 ISSN: 2587-2680 e-ISSN: 2587-246X Publisher: Sivas Cumhuriyet University

Eco-Friendly and Durable Sponge with In Situ Formed Silver Nanoparticles for Antimicrobial Filtration

Furkan Sahin [1,a,*]

[1] *Department of Biomedical Engineering, Faculty of Engineering and Architecture, Beykent University, 34398, Istanbul, Türkiye*

**Corresponding author*

Research Article

History
Received: 09/03/2024
Accepted: 15/05/2025

ABSTRACT

Microbial contamination poses a significant challenge to the management of water resources and biomedical applications. In this study, the development of a biogenic antimicrobial filtration system has been successfully achieved. This system utilizes a plant extract-mediated synthesis approach for in situ formation of silver nanoparticles (AgNPs) within a porous sponge matrix. The fabrication process involved the immersion of a commercial sponge in an aqueous solution of $AgNO_3$ and plant extract, followed by a thermal treatment. The structural and chemical properties of the Ag@Sponge were then confirmed via a range of analytical methods, including scanning electron microscopy (SEM), energy-dispersive X-ray spectroscopy (EDX), X-ray diffraction (XRD), and X-ray photoelectron spectroscopy (XPS). These results indicated the successful incorporation of AgNPs within the sponge, with a predominant spherical morphology and an average size of 54 ± 14 nm. Antimicrobial activity tests demonstrated that Ag@Sponge exhibited significant bacterial and fungal inactivation, achieving >99.99999% microbial reduction against *Escherichia coli* (*E. coli*), *Staphylococcus aureus* (*S. aureus*), and *Candida albicans* (*C. albicans*) (R > 7). Furthermore, the results of filtration experiments demonstrated that microbial removal efficiency increased progressively over six cycles, reaching final reductions of 6.2–6.4 log CFU/mL for *E. coli*, *S. aureus*, and *C. albicans*. Mechanical durability tests confirmed that Ag@Sponge retained >6 log CFU/mL reduction after 5000 cm abrasion (down to 6.6 ± 0.5) and 400 bending cycles (down to 6.1 ± 1.2), indicating strong mechanical resilience and in situ nanoparticle stability. These findings highlight the potential of Ag@Sponge as a sustainable and efficient antimicrobial filtration material for practical applications in water purification and medical decontamination.

Keywords: Disinfection, Green fabrication, Ag nanoparticles, Antimicrobial, Sponge.

[a] *furkansahin@beykent.edu.tr* *https://orcid.org/0000-0001-5409-3925*

Introduction

Microbial contamination continues to pose a significant challenge to the sustainable management of water resources and biomedical applications [1]. Hospital-based liquid waste, in particular, poses considerable risks to both the environment and public health due to its high levels of pathogenic microorganisms, antibiotic residues, and pharmaceutical components [2,3]. Inadequate treatment of such waste accelerates the spread of antibiotic resistance and causes irreversible damage to ecosystems [1]. The World Health Organization (WHO) reports that approximately 1.5 million people die each year from complications related to diseases originating from unsafe water sources, and that antibiotic resistance further exacerbates this situation [4]. In response, the United Nations (UN) has emphasized the importance of safe water resource management and pathogen load reduction through Sustainable Development Goal 6 (Clean Water and Sanitation) and Sustainable Development Goal 3 (Good Health and Well-being) within the broader framework of the Sustainable Development Goals (SDGs) [5,6]. In this context, the development of low-cost and sustainable disinfection technologies that do not leave antibiotic residues has become a global necessity [7].

A review of the extant literature reveals a plethora of methodologies for liquid disinfection, including chlorination, ozonation and UV radiation, which are notable for their strong oxidation effects [8–10]. However, a significant disadvantage of these methods is that by-products formed during disinfection (e.g., chlorinated organic compounds) can cause secondary pollution, resulting in environmental toxicity and health risks [8,9]. This situation highlights the necessity for the development of alternative strategies [8]. In recent years, the integration of antimicrobial materials into disinfection systems has emerged as an innovative approach [11,12], but certain disadvantages persist, including the risk of antibiotic or chemical residues in the liquid and the limited effectiveness against diverse microorganisms [13]. An alternative and more sustainable approach involves the incorporation of metallic nanoparticles, known for their broad-spectrum antimicrobial properties, into filtration systems [14]. Metal nanoparticles have been shown to exhibit high activity against microorganisms and to enhance the performance of disinfection systems through mechanisms such as the production of reactive oxygen species and the disruption of cell membranes [15–17]. AgNPs in particular have a proven track record of

effectiveness and reliability over time [15]. In contrast to essential metals such as copper, silver is not required for bacterial physiology and therefore lacks associated homeostatic regulation [15]. As a result, Ag^+ ions irreversibly bind to critical thiol-containing biomolecules, including cysteine residues in enzymes and membrane proteins, leading to irreversible enzyme inactivation and disruption of respiratory electron transport chains [15]. Furthermore, the catalytic generation of reactive oxygen species (ROS), particularly H_2O_2, contributes to oxidative stress and further compromises bacterial viability [15,17]. The synergy of these characteristics results in AgNPs demonstrating exceptional potency at low concentrations, while concurrently minimizing the risk of resistance development. This positions silver as one of the most efficient and reliable antimicrobial agents among metallic nanoparticles.

Nonetheless, a number of fundamental issues inherent in systems developed with metal nanoparticles have yet to be resolved. Chief among these is the propensity of nanoparticles to readily detach from the carrier surface [18], a phenomenon that precipitates a swift decline in the efficiency of the filtration system [19]. Moreover, the utilization of chemical reagents in nanoparticle production has the potential to engender environmental toxicity and escalate production costs [20–22]. Consequently, there is a compelling imperative to explore the development of cost-effective, sustainable, and high-performance materials that are synthesized in an environmentally friendly manner [23].

The present study set out to cultivate AgNPs directly on the surface of a sponge by means of an eco-friendly method that utilized plant extracts. Almond shell extracts were employed as a means to reduce Ag ions and stabilize nanoparticles, a process that is environmentally friendly and reduces reliance on chemical reagents. It is well established that such plant-based reductants contain polyphenols, flavonoids and organic acids, which facilitate the reduction of metal ions and provide surface functional groups for stabilization [21]. In the preceding literature, a number of plant sources, including tea leaves, citrus peels and other agricultural residues, have been documented for analogous purposes [16,21]. However, the present study elected to utilize almond shells on the basis of their elevated phenolic content, local availability and potential for valorization as a waste-derived material [24]. The sponge was used as a carrier matrix for nanoparticles due to its high surface area and durability. This approach resulted in the development of a low-cost, sustainable and durable filtration system. The Ag@Sponge material was thoroughly characterized using a range of analytical techniques, including scanning electron microscopy (SEM), X-ray diffraction (XRD), and X-ray photoelectron spectroscopy (XPS). Furthermore, the material's effectiveness in reducing microbial load in liquid waste and its long-term performance was comprehensively investigated.

Materials and Methods

Fabrication of Ag@Sponge

The Ag@Sponge platform was synthesized through a strategy of in situ growth of Ag nanostructures on the sponge surface. The synthesis process involved a biogenic reduction method that was used in an environmentally friendly manner, with almond shell extract serving as the reducing agent of choice.

To prepare the almond shell extract, 10 g of washed and dried almond shell at 40 °C was kept in 100 mL of double distilled water at 80 °C for 6 hours. The resulting solution was then filtered using a filter paper (M&Nagel MN 640 m, pore size 4–12 µm, medium flow rate) to remove solid content, thereby yielding the aqueous almond shell extract. The prepared almond shell extract was then utilized for the reduction of Ag ions and the formation of Ag@Sponge. To this end, a 1.5 mM $AgNO_3$ aqueous solution was prepared and 20 mL of $AgNO_3$ solution and 10 mL of almond extract were added to a 50 mL Falcon tube, resulting in a final solution concentration of 1 mM. Thereafter, the sponge sample was placed in the solution and gently shaken to ensure homogeneous distribution. In situ AgNPs growth was then performed by keeping the tube in a water bath at 90 °C for 1 hour. Subsequent to the completion of the process, the sponge sample was removed from the solution and dried in an oven at 50 °C, resulting in the formation of a platform that was designated Ag@Sponge.

Characterization of Ag@Sponge

Morphological analysis of the produced nanostructured Ag@Sponge and the control surface was performed using a scanning electron microscope (SEM, Zeiss EVO LS10, 25 kV). In order to determine the composition of the surface, elemental analysis was performed with energy dispersive X-ray spectroscopy (EDX, XFlash 6110, Bruker) integrated into the SEM system. The size distribution of the particles on the surface was calculated using ImageJ software from the obtained SEM images. The chemical composition and bonding structure of the produced surfaces were analyzed using X-ray photoelectron spectroscopy (XPS, K-alpha, Thermo Scientific) equipped with a monochromatic Al Kα (1486.7 eV) X-ray source. X-ray diffraction (XRD) analysis was performed to examine the crystal structure, and the measurements were performed with the Panalytical Empyrean XRD system at 45 kV and 40 mA operating conditions, using Cu K-α1 (λ = 1.5406 Å) X-ray source. The XRD data were processed using OriginPro (OriginLab Corp., USA), with a 100-point Savitzky-Golay smoothing algorithm applied in order to reduce noise and enhance peak clarity without distorting peak shape. The average size of the crystallites was calculated from the XRD data using the Debye–Scherrer equation (Eq. 1).

$$D = \frac{K * \lambda}{\beta * cos\theta} \quad (1)$$

In this calculation, the Bragg angle (θ), X-ray wavelength (λ) and full width at half maximum (FWHM) peak width (β) parameters were used. The degree of crystallinity (CI) was calculated by taking the ratio of the crystalline peak areas within the total area under the diffraction curve (Eq. 2).

$$CI = \frac{Area\ of\ all\ the\ crystalline\ peaks}{Area\ of\ all\ the\ crystalline\ and\ amorhpous\ peaks} \quad (2)$$

Antimicrobial Assay

Antimicrobial, antibacterial and antifungal activity were evaluated by following the AATCC test protocol with slight modifications. Bactericidal activity was investigated on Gram-negative *E. coli* (ATCC 25922) and Gram-positive *S. aureus* (ATCC 25923) bacteria, while fungicidal activity was tested on *C. albicans*. Mueller-Hinton liquid (broth) and solid (agar) media were utilized for bacterial strains, while Sabouraud Dextrose Broth and Sabouraud Dextrose Agar were employed for fungal strains. 100 µL each of fungal and bacterial suspension at 0.5 McFarland turbidity was taken and inoculated onto Ag@Sponge and control surfaces of approximately 1 × 1 cm² in size. Untreated sponge was used as the control surface. After 24 hours of incubation at 37 °C, the surfaces were placed in 10 mL of PBS and 5 minutes of sonication and 5 minutes of vortexing were applied to transfer the microorganisms on the surfaces to the PBS medium. A volume of 100 µL of the resulting suspension was then inoculated onto solid media, after which the number of colonies on agar plates was enumerated following a 24-hour incubation period at 37 °C. The antimicrobial activity was then calculated according to equation 3.

$$Antimicrobial\ Activity\ (R) = log(Ut) - log(At) \quad (3)$$

In this equation, *At* represents the average number of colonies surviving on the developed Ag@Sponge platform, while *Ut* represents the average number of colonies surviving on the untreated sponge.

Microbial Retention and Inactivation Performance Test

In order to evaluate the performance of microbial filtration of the Ag@Sponge platform, the microorganism *E. coli*, *S. aureus* and *C. albicans* were utilized. The microorganism suspensions were prepared in sterile phosphate-buffered saline (PBS) by adjusting to 1 McFarland turbidity standard. A total of 20 mL of PBS solution was used for each microorganism.

The prepared PBS-microorganism suspension was then passed through sponge samples that had been prepared in advance at a flow rate of 2 mL/min. The liquid that had been filtered was collected in a sterile beaker, and the sponge was left for one hour to ensure that the liquid absorbed by the sponge was completely released. At the conclusion of this period, the final liquid retained by the sponge, which did not drip freely, was added to the filtrate collected in the beaker by gently compressing the sponge. 100 µL of the waste liquid accumulated in the beaker after filtration was taken and inoculated on solid medium and incubated at 37 °C for 24 hours. The microorganism retention and inactivation performance were then evaluated by taking wastewater and restarting the filtration process. This procedure was repeated six times. After each filtration cycle, the colonies formed on the solid media were counted and the number of microorganisms removed was compared to the initial microorganism load using Equation 3.

Antimicrobial Robustness Test

In order to evaluate the durability of the produced samples in the context of antimicrobial activity under mechanical stress, a series of abrasion and bending tests were conducted. The abrasion test involved subjecting the samples to friction against an aluminum foil surface over specific distances, with a weight of approximately 200 g applied. The samples were shifted by 500 cm, 1000 cm, 2500 cm and 5000 cm to assess the impact of surface abrasion and material erosion on their antimicrobial activity. The bending test involved subjecting the samples to repeated bending cycles, with the number of cycles ranging from 50 to 400, to simulate the durability of the sponges under mechanical loads such as tension and flexion. Following each test stage, the samples were subjected to antimicrobial tests, as outlined in section 2.3, to evaluate the effect of mechanical stresses on microorganism inhibition capacity.

Results and Discussion

A biogenic antimicrobial filtration system was developed through a plant extract-mediated synthesis approach for the in situ formation of AgNPs within a porous sponge matrix (Figure 1A). The fabrication process involved the immersion of a commercial sponge in an aqueous solution of $AgNO_3$ and plant extract, followed by a thermal treatment at 90°C for 60 minutes. The color change from pale yellow to dark brown indicated the successful reduction of Ag^+ ions and in situ formation of AgNPs. To evaluate the potential application of Ag@Sponge in microbial filtration, a conceptual schematic is presented in Figure 1B. Contaminated liquid waste passes through the Ag@Sponge, where microbial retention and inactivation occur due to the antimicrobial properties of AgNPs, resulting in a disinfected liquid effluent.

The morphological characteristics of the pristine sponge and Ag@Sponge were examined using scanning electron microscopy (SEM) (Figure 1C). While the unmodified sponge exhibited a clean and uniform porous structure, the Ag@Sponge showed embedded nanoparticles throughout the surface, as highlighted in the magnified regions. SEM images revealed that the nanoparticles on the surface were predominantly spherical; however, spiky structures were also observed in certain regions (e.g. area marked yellow). The distribution

of the particles was found to be nonuniform, with partial aggregations evident as surface clusters. This morphology is attributed to the spontaneous and progressive reduction of metal ions directly on the substrate, where nucleation occurs randomly and continues over time, which is typically observed in similar in situ formation processes [16,25]. Consequently, the newly formed nanoparticles have the capacity to emerge on top of existing ones, thus giving rise to the formation of layered or aggregated structures. The particle size distribution, based on distinguishable spherical domains within these aggregates, revealed an average diameter of 54 ± 14 nm (Figure 1D). The presence of Ag in the modified sponge was further confirmed by EDX analysis (Figure 1E). A comparison of the spectrum of the pristine sponge, primarily composed of carbon and oxygen [26], with that of the Ag@Sponge revealed the presence of additional peaks corresponding to Ag (15.6 wt%), along with minor contributions from Na, K, and Cl, which may have originated from the almond shell extract [24]. The findings, when considered collectively, indicate the successful synthesis of Ag@Sponge via a green chemistry approach, with its structural and chemical properties supporting its potential use in antimicrobial liquid filtration applications.

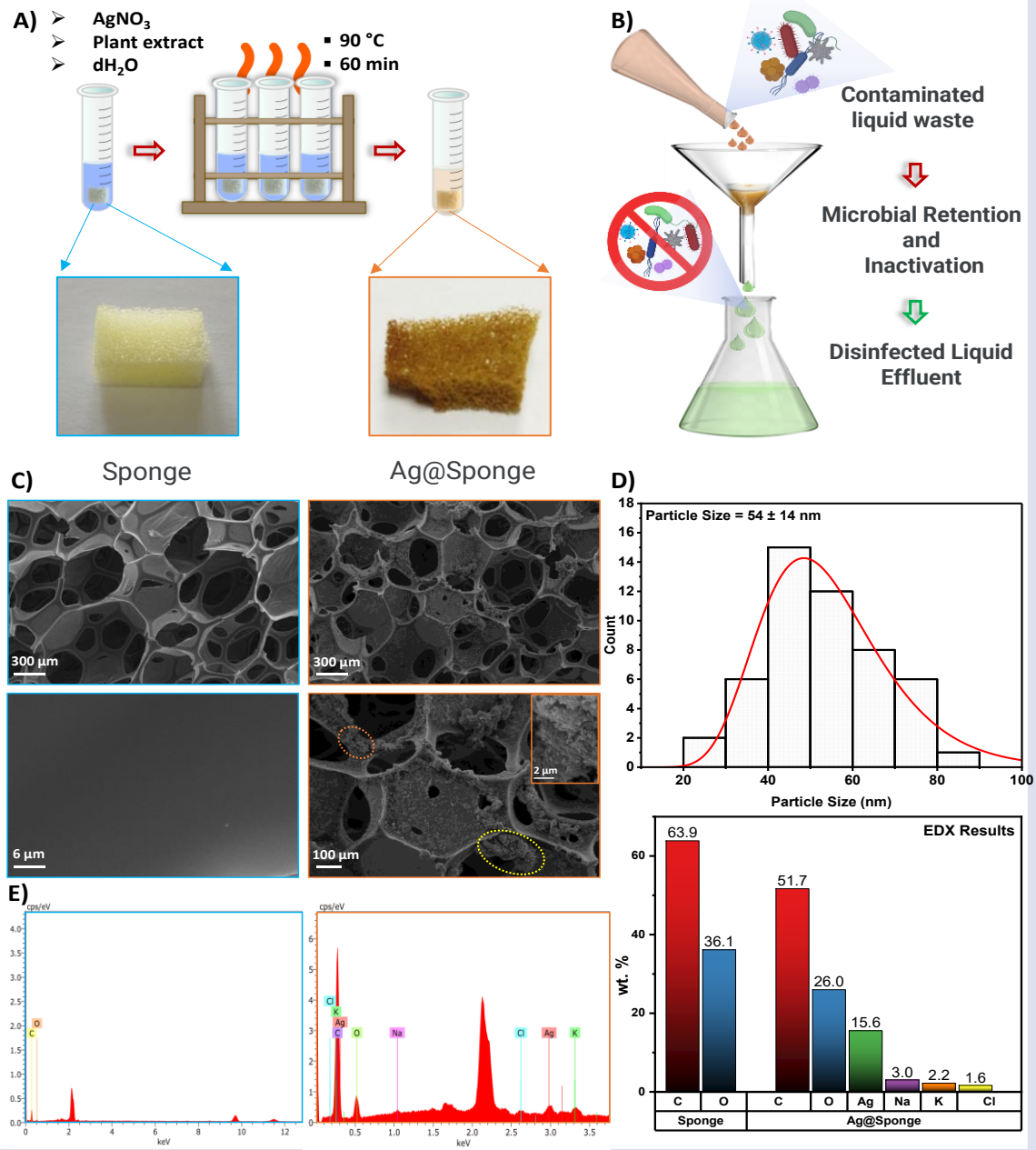

Figure 1. Schematic representation of the process of in situ formation of AgNPs on the sponge (A) and the disinfection of contaminated liquid waste using the developed Ag@Sponge (B). SEM images (C), particle size distribution graph (D), and EDX results (E) of the sponge and Ag@Sponge.

EDX results confirmed exclusively the presence of Ag; however, they did not provide any information regarding its chemical state or crystalline form. Therefore, XRD and XPS analyses were conducted to elucidate the structural and chemical characteristics of Ag within the sponge matrix.

In order to investigate the crystalline structure of the AgNPs incorporated into the sponge matrix, XRD analysis was performed. As demonstrated in Figure 2A, characteristic diffraction peaks were identified at 2θ = 38.1°, 44.2°, 64.8°, 77.3°, and 81.2°, which correspond to the (111), (200), (220), (311), and (222) planes of face-centered cubic (fcc) metallic silver (Ag^0) (JCPDS #No. 04-0783) [27]. The presence of these peaks confirmed the successful formation of metallic Ag within the porous sponge structure. The average crystallite size of the AgNPs was determined using the Debye–Scherrer equation, based on the full width at half maximum (FWHM) of the peaks, yielding average crystallite sizes of 6.5 nm (111), 5.1 nm (200), 5.1 nm (220), 5.4 nm (311), and 4 nm (222) for the respective diffraction peaks. A comparison of these values with those of previously reported monometallic AgNPs synthesized via green chemistry approaches suggests that the former exhibit a relatively smaller crystal size distribution [27,28]. This reduction in crystallite size can be attributed to the specific synthesis conditions, including the interaction of silver precursors with the sponge matrix. It is hypothesized that this interaction may have influenced the nucleation rate and inhibited the growth of larger crystallites [29]. The selection of the matrix and the growth environment is likely to have played a crucial role in limiting the crystal size [29], resulting in a higher surface-to-volume ratio that is often desirable for applications such as catalysis and antimicrobial activity [30]. Furthermore, the crystallinity index (CI) was calculated as 25.24%. CI values exceeding 40% have been reported for certain bimetallic and trimetallic nanoparticle systems [16]. Nevertheless, direct comparison is constrained by the disparities in substrate materials and synthesis conditions.

To further confirm the chemical state of Ag in the synthesized Ag@Sponge, high-resolution XPS analysis was conducted; the Ag 3d spectrum (Figure 2B) exhibiting two prominent peaks at binding energies of 368.3 eV and 374.3 eV, corresponding to Ag $3d_{5/2}$ and Ag $3d_{3/2}$, respectively. The observed spin-orbit splitting of 6.0 eV was in good agreement with literature reports for metallic silver (Ag^0) [27,31], confirming that the silver present in the sponge was in its reduced, elemental form rather than in an oxidized state. These XPS results are consistent with the XRD findings, reinforcing the conclusion that AgNPs were successfully synthesized and incorporated into the sponge matrix through the plant extract-mediated reduction of Ag^+ ions.

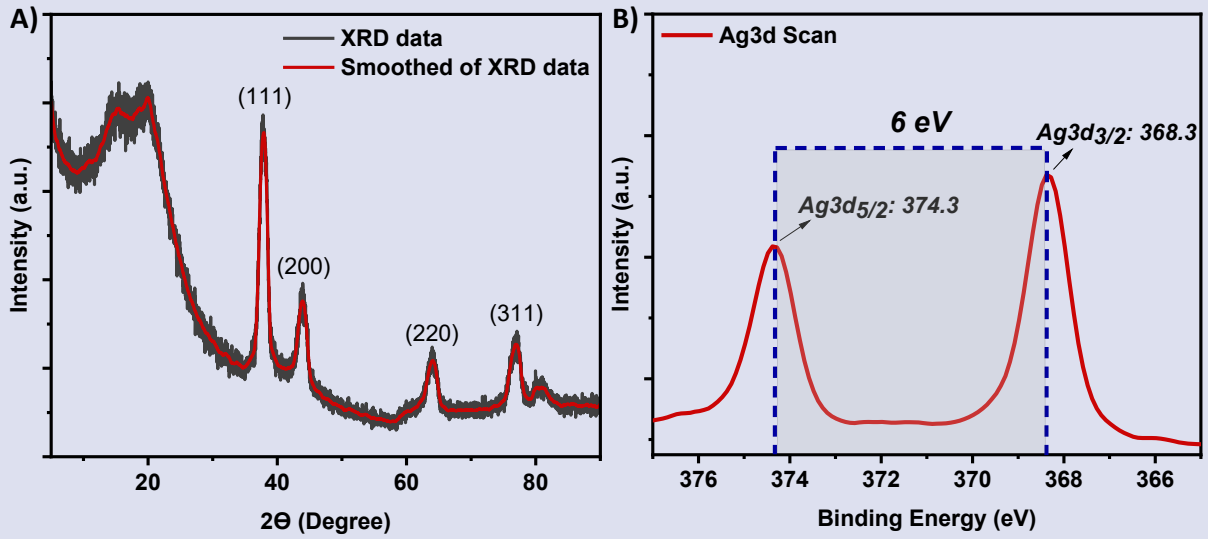

Figure 2. Chemical characterization of the Ag@Sponge platform. A) XRD patterns of Ag@Sponge. B) High-resolution XPS spectra of Ag 3d in Ag@Sponge.

The antimicrobial activity of Ag@Sponge was evaluated against a range of common pathogenic microorganisms, including the Gram-positive bacteria *S. aureus*, the Gram-negative bacteria *E. coli*, and the fungal pathogen *C. albicans*. According to the test results, Ag@Sponge effectively inactivated nearly all inoculated microorganisms. In comparison with the untreated sponge material, Ag@Sponge demonstrated logarithmic reductions (R) of 7.2 ± 0.2, 7.6 ± 0.3, and 7.5 ± 0.2 against *E. coli*, *S. aureus*, and *C. albicans*, respectively. The R value, which is indicative of antimicrobial efficacy, significantly exceeded the critical threshold of 2 [32], indicating an inactivation rate of >99.99999%. It is noteworthy that Ag@Sponge exhibited higher antibacterial efficacy against Gram-positive bacteria compared to Gram-negative bacteria. This phenomenon can be attributed to the structural differences in their cell walls. Gram-positive bacteria possess a thick peptidoglycan layer, whereas Gram-negative bacteria have an additional outer membrane composed of phospholipids and

polysaccharides that surrounds the peptidoglycan layer [33], This outer membrane may act as a barrier, limiting the penetration of metallic nanoparticles into the bacterial cell, thereby reducing bactericidal efficacy. In addition, inorganic oxide nanoparticles exhibit a heightened adsorption affinity for distinctive components within the cell wall of Gram-positive bacteria, including teichoic acids, predominantly via π-π interactions [34]. Differences in the isoelectric points of their membranes result in Gram-negative *E. coli* having a less negative surface charge compared to Gram-positive *S. aureus* [35], which may contribute to the enhanced inhibitory activity of metallic nanoparticles against Gram-positive bacteria [16]. However, it is important to note that the calculated R values are relative to the control surface, and variations in microbial growth on the control samples could influence the final antimicrobial efficacy values.

Beyond its antibacterial effects, Ag@Sponge also exhibited excellent antifungal activity against *C. albicans*, a leading cause of nosocomial infections. One possible mechanism underlying this strong antimicrobial activity is the ability of AgNPs to enhance reactive oxygen species (ROS) generation, leading to oxidative stress-induced apoptosis [35]. The generation of ROS by metallic nanoparticles is known to cause oxidative damage to microbial cells through mechanisms such as DNA/RNA strand breakage, protein oxidation, membrane disruption, and lipid peroxidation, ultimately leading to cell death [25,35]. Additionally, Ag ions released from the nanoparticles have the capacity to penetrate cells via ion channels and/or purines, bind to lipopolysaccharides, peptidoglycans, and carboxyl groups, and alter the electrochemical potential of intracellular and extracellular components [36]. This can result in membrane depolarization and instability, leading to nuclear membrane deformation, cytoplasmic leakage, and damage to essential cellular processes, including DNA replication and transcription [17,36]. Furthermore, the nanoscale spherical morphology of the AgNPs likely enhanced the antimicrobial effect due to their high surface area-to-volume ratio, which promotes greater interaction with microbial cells [37]. In summary, the potent antimicrobial activity observed in Ag@Sponge is most likely a consequence of nano/micro-scale metallic particles encountering pathogens, disrupting cell membranes, penetrating microbial cells, and interfering with critical biomolecular structures such as proteins and DNA.

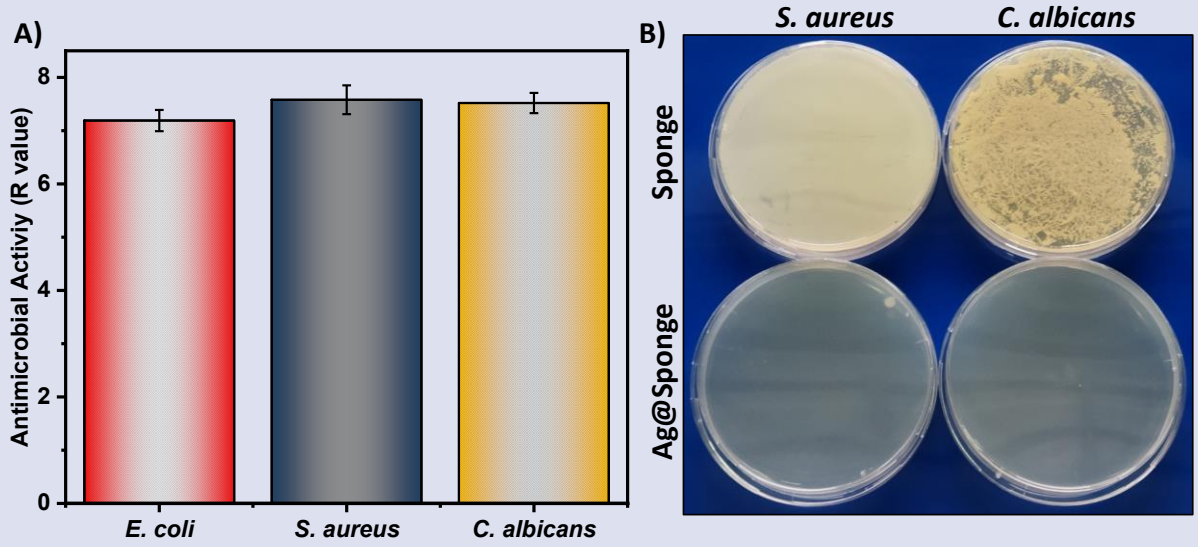

Figure 3. (A) Antimicrobial activity of Ag@Sponge against E. coli, S. aureus, and C. albicans. (B) Photographs demonstrating the comparative microbial growth on untreated sponge (control) and Ag@Sponge surfaces.

The microbial removal performance of the developed Ag@Sponge material was evaluated using a simple filtration setup (Figure 1B and 4). The results demonstrate that microbial removal gradually increases with the filtration process, with a significant removal observed for all microorganism species in the first filtration stage, resulting in a decrease of approximately >4 log CFU/mL in all microbial strains. As the number of filtrations increased, the removal rate continued to increase, although at a rate that was lower compared to the first filtration.

This phenomenon can be attributed to the combined impact of multiple factors during the filtration process. Initially, microorganisms interact with the Ag@Sponge surface, resulting in a rapid removal due to the high surface activity of AgNPs [38]. Additionally, the initial stage of filtration facilitates the retention of free and large microorganism clusters in the suspension, contributing to an enhanced filtration efficiency. However, as the filtration progresses, the removal rate becomes more limited due to a decrease in the concentration of microorganisms remaining in the system. Furthermore, the accumulation of microbial residues and biological materials on the surface may partially reduce the binding areas of new microorganisms [38]. Additionally, due to the controlled release of silver ions (Ag^+), the more intense

effect of free ions in the initial stages may cause this interaction to gradually balance in the subsequent cycles [39].

In the final filtration stage, microbial removal was achieved at approximately 6-7 log CFU/mL levels in the 6th cycle, and it was revealed that the Ag@Sponge material offers high and stable antimicrobial activity. These results show that the developed sponge-based filter material exhibits effective performance in multi-stage filtrations and offers a strong alternative for the removal of microbial contamination.

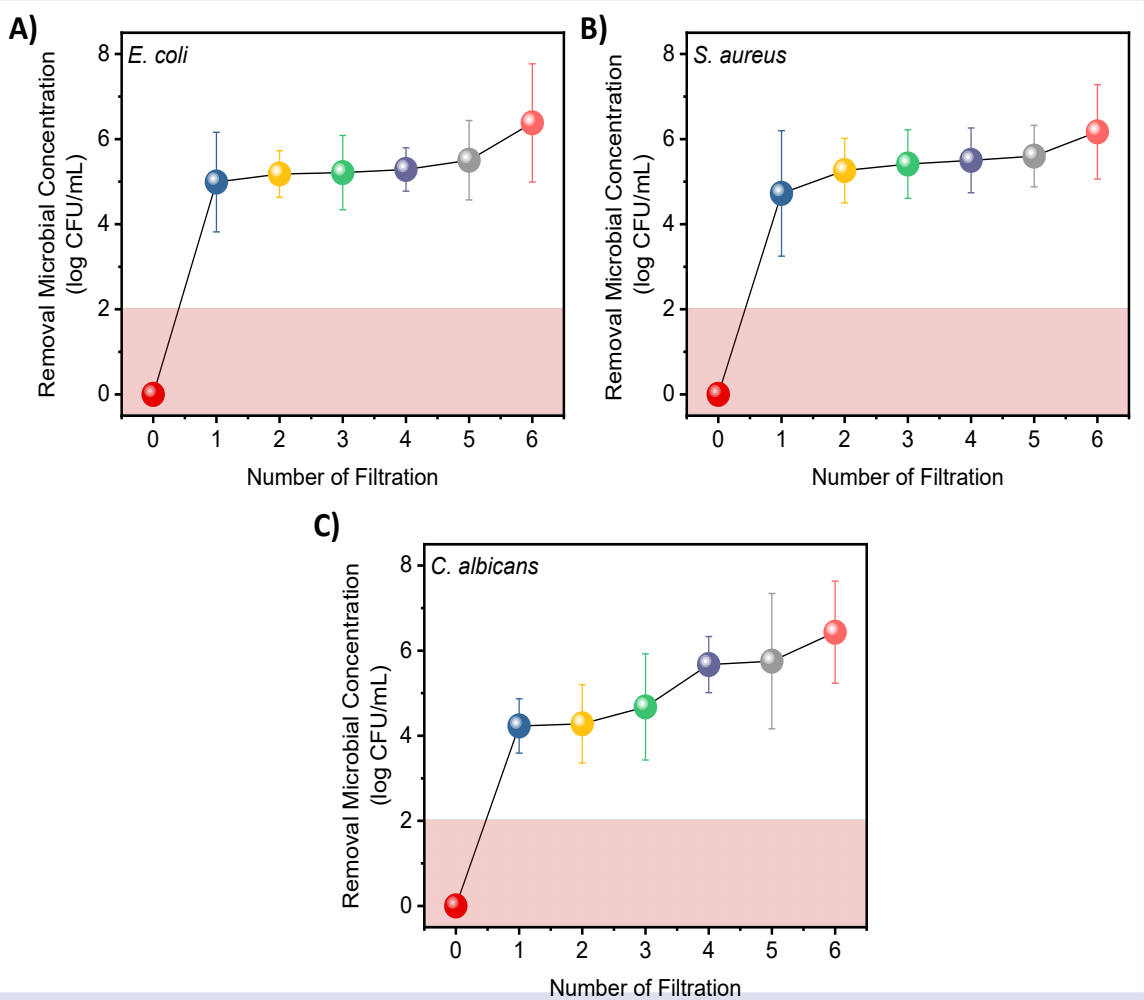

Figure 4. Filtration performance of the developed Ag@Sponge material on A) *E. coli,* B) *S. aureus* and C) *C. albicans* microorganisms. Microbial removal concentration (log CFU/mL) was investigated throughout the filtration cycle. The shaded red area in the figure represents the safe limit zone required for microbial filtration.

The long-term effectiveness of materials utilized in filtration processes is contingent not only on their antimicrobial performance but also on their mechanical strength and structural stability. In this context, the antimicrobial activity preservation performance of the developed Ag@Sponge material was evaluated following abrasion and bending tests (Figure 5).

As demonstrated in Figure 5A, the R value exhibited minimal decline against *E. coli*, *S. aureus*, and *C. albicans* microorganisms across the range of abrasion distances from 500 cm to 5000 cm. The material's initial high antimicrobial activity was retained, suggesting that the AgNPs on the Ag@Sponge surface maintained strong bonding against mechanical effects and did not readily separate from the material surface. The bending strength test results, presented in Figure 5B, demonstrate that after 50 to 400 bending cycles, the antimicrobial activity against all microorganisms was significantly preserved. Notably, even after 400 bending cycles, the decrease in the R value was minimal, and it was observed that the flexibility properties of the material did not have a negative impact on the antimicrobial activity. This outcome demonstrates that the Ag@Sponge material possesses a flexible and durable structure, capable of retaining its functionality under mechanical stresses. In general, the results of the abrasion and bending tests demonstrate that the developed Ag@Sponge material exhibits a level of robustness (mechanical durability) that renders it suitable for long-term use. This feature confirms that the material can provide sustainable antimicrobial activity in real-life applications and can demonstrate stable performance in repeated filtration processes [40].

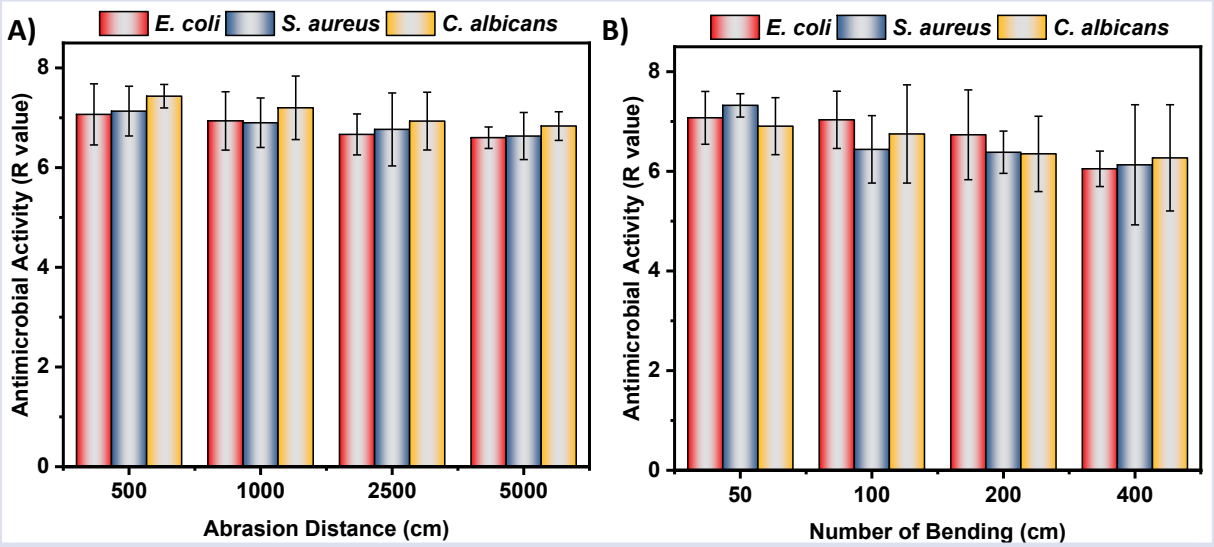

Figure 5. Preservation performance of antimicrobial activity under mechanical strength of the developed Ag@Sponge material. (A) Antimicrobial activity (R value) against *E. coli*, *S. aureus* and *C. albicans* microorganisms after different abrasion distances (500–5000 cm). (B) Evaluation of antimicrobial activity after different bending cycles (50–400 times).

Conclusion

In this study, a biogenic antimicrobial filtration system, Ag@Sponge, was successfully synthesized via a green chemistry approach utilizing plant extract-mediated formation of AgNPs. The utilization of almond shell extract facilitated the in situ formation of AgNPs within a porous sponge matrix, thereby obviating the requirement for hazardous chemical reagents and ensuring a sustainable fabrication process. Structural analysis confirmed the effective incorporation of AgNPs into the porous sponge matrix, while antimicrobial tests demonstrated exceptional efficacy against bacterial and fungal pathogens, achieving microbial inactivation rates exceeding 99.99%. The filtration experiments further validated the system's effectiveness, demonstrating significant microbial removal across multiple filtration cycles (R>6). Additionally, mechanical durability assessments confirmed that Ag@Sponge retained its antimicrobial properties even after extensive abrasion and bending tests. The material's sustained antimicrobial activity and structural robustness position it as a promising candidate for real-world water purification and biomedical applications. The findings highlight the potential of Ag@Sponge as a cost-effective and environmentally friendly solution for microbial contamination in liquid waste treatment systems. Future studies may focus on optimizing the material's scalability, regeneration capabilities, and real-world performance under complex environmental conditions.

Conflict of Interest

There are no conflicts of interest in this work.

Acknowledgment

This study did not receive funding from any public, commercial, or non-profit organizations.

References

[1] Abosse J.S., Megersa B., Zewge F., Eregno F.E., Healthcare waste management and antimicrobial resistance: a critical review, *Journal of Water and Health*, 22 (2024) 2076–2093.

[2] Chand S., Shastry S., Hiremath S., Joel J., Bhat C., Uday V., Water, sanitation, hygiene and biomedical waste disposal in the healthcare system: A review, *Biomedicine*, 40 (2020) 14.

[3] Singh H., YT K., Mishra A.K., Singh M., Mohanto S., Ghumra S., Seelan A., Mishra A., Kumar A., Pallavi J., Ahmed M.G., Sangeetha J., Thangadurai D., Harnessing the foundation of biomedical waste management for fostering public health: strategies and policies for a clean and safer environment, *Discov Appl Sci*, 6 (2024) 89.

[4] Pal M., Ayele Y., Hadush A., Panigrahi S., Jadhav V., Public Health Hazards Due to Unsafe Drinking Water, *Air Water Borne Dis.*, 7 (2018) 1000138.

[5] Matta G., Kumar P., Uniyal D.P., Joshi D.U., Communicating Water, Sanitation, and Hygiene under Sustainable Development Goals 3, 4, and 6 as the Panacea for Epidemics and Pandemics Referencing the Succession of COVID-19 Surges, *ACS EST Water*, 2 (2022) 667–689.

[6] Tyagi I., Kumar V., Tyagi K., Water pollution—sources and health implications of the environmental contaminants on the aquatic ecosystem and humans: approach toward sustainable development goals, In: Dehghani M.H., Karri R.R., Tyagi I., Scholz M. (Eds.), Water, The Environment, and the Sustainable Development Goals, 1st ed. Elsevier, (2024) 35–66.

[7] Rajapakse J., Otoo M., Danso G., Progress in delivering SDG6: Safe water and sanitation, *Cambridge Prisms: Water*, 1 (2023) e6.

[8] Bharti B., Li H., Ren Z., Zhu R., Zhu Z., Recent advances in sterilization and disinfection technology: A review, *Chemosphere*, 308 (2022) 136404.

[9] Da Costa J.B., Rodgher S., Daniel L.A., Espíndola E.L.G., Toxicity on aquatic organisms exposed to secondary effluent disinfected with chlorine, peracetic acid, ozone and UV radiation, *Ecotoxicology*, 23 (2014) 1803–1813.

[10] Kong J., Lu Y., Ren Y., Chen Z., Chen M., The virus removal in UV irradiation, ozonation and chlorination, *Water Cycle*, 2 (2021) 23–31.

[11] Mandal T.K., Nanomaterial-Enhanced Hybrid Disinfection: A Solution to Combat Multidrug-Resistant Bacteria and Antibiotic Resistance Genes in Wastewater, *Nanomaterials*, 14 (2024) 1847.

[12] Cai Y., Sun T., Li G., An T., Traditional and Emerging Water Disinfection Technologies Challenging the Control of Antibiotic-Resistant Bacteria and Antibiotic Resistance Genes, *ACS EST Eng.*, 1 (2021) 1046–1064.

[13] Sanganyado E., Gwenzi W., Antibiotic resistance in drinking water systems: Occurrence, removal, and human health risks, *Science of The Total Environment*, 669 (2019) 785–797.

[14] Castro-Muñoz R., The Role of New Inorganic Materials in Composite Membranes for Water Disinfection, *Membranes*, 10 (2020) 101.

[15] Slavin Y.N., Asnis J., Häfeli U.O., Bach H., Metal nanoparticles: understanding the mechanisms behind antibacterial activity, *J Nanobiotechnol*, 15 (2017) 65.

[16] Demirel Sahin G., Sahin F., Barlas F.B., Onses M.S., Acar S., Antimicrobial, anti-biofouling, antioxidant, and biocompatible fabrics with high durability via green growth of trimetallic nanoparticles, *Materials Today Communications*, 41 (2024) 110807.

[17] Sahin F., Camdal A., Demirel Sahin G., Ceylan A., Ruzi M., Onses M.S., Disintegration and Machine-Learning-Assisted Identification of Bacteria on Antimicrobial and Plasmonic Ag–CuxO Nanostructures, ACS Appl. Mater. *Interfaces*, 15 (2023).

[18] Carrillo J.-M.Y., Dobrynin A.V., Contact Mechanics of Nanoparticles, *Langmuir*, 28 (2012) 10881–10890.

[19] Wang H., Zhang W., Zeng S., Shen C., Jin C., Huang Y., Interactions between nanoparticles and fractal surfaces, *Water Research*, 151 (2019) 296–309.

[20] Besha A.T., Liu Y., Bekele D.N., Dong Z., Naidu R., Gebremariam G.N., Sustainability and environmental ethics for the application of engineered nanoparticles, *Environmental Science & Policy*, 103 (2020) 85–98.

[21] Saravanan A., Kumar P.S., Karishma S., Vo D.-V.N., Jeevanantham S., Yaashikaa P.R., George C.S., A review on biosynthesis of metal nanoparticles and its environmental applications, *Chemosphere*, 264 (2021) 128580.

[22] Kirubakaran D., Wahid J.B.A., Karmegam N., Jeevika R., Sellapillai L., Rajkumar M., SenthilKumar K.J., A Comprehensive Review on the Green Synthesis of Nanoparticles: Advancements in Biomedical and Environmental Applications, *Biomedical Materials & Devices*, (2025) 1-26.

[23] Wei F., Zhao X., Li C., Han X., A novel strategy for water disinfection with a AgNPs/gelatin sponge filter, *Environ Sci Pollut Res*, 25 (2018) 19480–19487.

[24] Queirós C.S.G.P., Cardoso S., Lourenço A., Ferreira J., Miranda I., Lourenço M.J.V., Pereira H., Characterization of walnut, almond, and pine nut shells regarding chemical composition and extract composition, *Biomass Conv. Bioref.*, 10 (2020) 175–188.

[25] Sahin F., Celik N., Ceylan A., Ruzi M., Onses M.S., One-step Green Fabrication of Antimicrobial Surfaces via In Situ Growth of Copper Oxide Nanoparticles, *ACS Omega*, 7 (2022) 26504–26513.

[26] Khan M.S.J., Kamal T., Ali F., Asiri A.M., Khan S.B., Chitosan-coated polyurethane sponge supported metal nanoparticles for catalytic reduction of organic pollutants, *International Journal of Biological Macromolecules*, 132 (2019) 772–783.

[27] Sahin F., Celik N., Camdal A., Sakir M., Ceylan A., Ruzi M., Onses M.S., Machine Learning-Assisted Pesticide Detection on a Flexible Surface-Enhanced Raman Scattering Substrate Prepared by Silver Nanoparticles, *ACS Appl. Nano Mater.*, 5 (2022) 13112–13122.

[28] Elemike E.E., Onwudiwe D.C., Fayemi O.E., Botha T.L., Green synthesis and electrochemistry of Ag, Au, and Ag–Au bimetallic nanoparticles using golden rod (Solidago canadensis) leaf extract, *Appl. Phys.*, A 125 (2019) 42.

[29] Meldrum F.C., O'Shaughnessy C., Crystallization in Confinement, *Advanced Materials,* 32 (2020) 2001068.

[30] Makvandi P., Wang C., Zare E.N., Borzacchiello A., Niu L., Tay F.R., Metal-Based Nanomaterials in Biomedical Applications: Antimicrobial Activity and Cytotoxicity Aspects, *Advanced Functional Materials*, 30 (2020) 1910021.

[31] Cheng D., Zhang Y., Liu Y., Bai X., Ran J., Bi S., Deng Z., Tang X., Wu J., Cai G., Wang X., Mussel-inspired synthesis of filter cotton-based AgNPs for oil/water separation, antibacterial and catalytic application, *Materials Today Communications*, 25 (2020) 101467.

[32] ISO 20743:2021, ISO (n.d.). https://www.iso.org/standard/79819.html (accessed March 8, 2025).

[33] Vaiwala R., Sharma P., Ganapathy Ayappa K., Differentiating interactions of antimicrobials with Gram-negative and Gram-positive bacterial cell walls using molecular dynamics simulations, *Biointerphases*, 17 (2022) 061008.

[34] Wang M., Li Z., Zhang Y., Li Y., Li N., Huang D., Xu B., Interaction with teichoic acids contributes to highly effective antibacterial activity of graphene oxide on Gram-positive bacteria, *Journal of Hazardous Materials*, 412 (2021) 125333.

[35] Modi S.K., Gaur S., Sengupta M., Singh M.S., Mechanistic insights into nanoparticle surface-bacterial membrane interactions in overcoming antibiotic resistance, *Front. Microbiol.*, 14 (2023) 1135579.

[36] Mikhailova E.O., Green Silver Nanoparticles: An Antibacterial Mechanism, *Antibiotics*, 14 (2025) 5.

[37] Duman H., Eker F., Akdaşçi E., Witkowska A.M., Bechelany M., Karav S., Silver Nanoparticles: A Comprehensive Review of Synthesis Methods and Chemical and Physical Properties, *Nanomaterials*, 14 (2024) 1527.

[38] Yu Y., Zhou Z., Huang G., Cheng H., Han L., Zhao S., Chen Y., Meng F., Purifying water with silver nanoparticles (AgNPs)-incorporated membranes: Recent advancements and critical challenges, *Water Research*, 222 (2022) 118901.

[39] Sukhorukova I.V., Sheveyko A.N., Shvindina N.V., Denisenko E.A., Ignatov S.G., Shtansky D.V., Approaches for Controlled Ag+ Ion Release: Influence of Surface Topography, Roughness, and Bactericide Content, *ACS Appl. Mater. Interfaces*, 9 (2017) 4259–4271.

[40] Saud A., Gupta S., Allal A., Preud'homme H., Shomar B., Zaidi S.J., Progress in the Sustainable Development of Biobased (Nano)materials for Application in Water Treatment Technologies, *ACS Omega*, 9 (2024) 29088–29113.